

Decoupling MSSM Higgs Sector and Heavy Higgs Decay

Tong Li

*ARC Centre of Excellence for Particle Physics at the Terascale,
School of Physics, Monash University, Melbourne, Victoria 3800, Australia*

Abstract

The decoupling limit in the MSSM Higgs sector is the most likely scenario in light of the Higgs discovery. This scenario is further constrained by MSSM Higgs search bounds and flavor observables. We perform a comprehensive scan of MSSM parameters and update the constraints on the decoupling MSSM Higgs sector in terms of 8 TeV LHC data. We highlight the effect of light SUSY spectrum in the heavy neutral Higgs decay in the decoupling limit. We find that the chargino and neutralino decay mode can reach at most 40% and 20% branching ratio, respectively. In particular, the invisible decay mode $BR(H^0(A^0) \rightarrow \tilde{\chi}_1^0 \tilde{\chi}_1^0)$ increases with increasing Bino LSP mass and is between 10%-15% (20%) for $30 < m_{\tilde{\chi}_1^0} < 100$ GeV. The leading branching fraction of heavy Higgses decay into sfermions can be as large as 80% for $H^0 \rightarrow \tilde{t}_1 \tilde{t}_1^*$ and 60% for $H^0/A^0 \rightarrow \tilde{\tau}_1 \tilde{\tau}_2^* + \tilde{\tau}_1^* \tilde{\tau}_2$. The branching fractions are less than 10% for $H^0 \rightarrow h^0 h^0$ and 1% for $A^0 \rightarrow h^0 Z$ for $m_A > 400$ GeV. The charged Higgs decays to neutralino plus chargino and sfermions with branching ratio as large as 40% and 60%, respectively. Moreover, the exclusion limit of leading MSSM Higgs search channel, namely $gg, b\bar{b} \rightarrow H^0, A^0 \rightarrow \tau^+ \tau^-$, is extrapolated to 14 TeV LHC with high luminosities. It turns out that the $\tau\tau$ mode can essentially exclude regime with $\tan\beta > 20$ for $L = 300$ fb $^{-1}$ and $\tan\beta > 15$ for $L = 3000$ fb $^{-1}$.

I. INTRODUCTION

The discovery of the Higgs boson at the LHC [1] raises two questions to theoretical particle physicists about the Higgs mechanism: is the discovered Higgs boson a pure Standard Model (SM) Higgs or SM-like Higgs from new physics theory? can the LHC prove or disprove new physics associated with Higgs sector? To answer these questions, it is important to investigate the implication of existing Higgs search data for extended Higgs sector in new physics framework and propose dedicated Higgs search signatures for experimentalists to test.

One of the best motivated theories beyond the SM is the weak scale supersymmetry (SUSY). In the framework of the Minimal Supersymmetric Standard Model (MSSM), unlike SM, the Higgs sector is composed of two Higgs doublets [2, 3]. After electroweak symmetry breaking, one has five physical Higgses, namely two CP-even Higgses h^0, H^0 , one CP-odd one A^0 and charged Higgses H^\pm . Between the two CP-even Higgs bosons, the one which couples to gauge bosons more strongly is SM-like. Moreover, the tree level Higgs masses are only determined by CP-odd Higgs mass parameter m_A and the ratio of two doublets' vacuum expectation values $\tan\beta$. Requiring the SM-like production cross sections of a Higgs boson of a 126 GeV mass with decay to diphoton and gauge bosons splits the MSSM Higgs parameters into two distinct regions [4]:

- (a) the “non-decoupling” region with $m_A \lesssim 130$ GeV and $\tan\beta < 10$ [5]. In this region, the heavy CP-even state H^0 is SM-like, while the light CP-even Higgs h^0 and the CP-odd one A^0 are nearly degenerate in mass and close to m_Z , and the charged state H^\pm is slightly heavier.
- (b) the “decoupling” region with $m_A \gtrsim 300$ GeV [5]. In this region, the light CP-even Higgs h^0 is SM-like, while all the other Higgs bosons are nearly degenerate with m_A [6].

The non-decoupling scenario leads to light non SM-like Higgs states which could be searched immediately without SUSY parameter dependence [7]. However, this scenario is highly constrained by both MSSM Higgs search bounds and b -quark rare decays [8]. The decoupling limit could thus be the most likely MSSM Higgs scenario in light of MSSM Higgs search results and the measurements of low-energy observables.

The leading channels probing decoupling scenario are the production of heavy neutral Higgses H^0, A^0 from gluon fusion, $b\bar{b}$ annihilation and associated process with b quarks in final state, followed by decay into $b\bar{b}$ or $\tau^+\tau^-$ [9]. In particular, with tau Yukawa coupling enhanced in large

$\tan\beta$ regime, the $\tau\tau$ decay mode puts the most stringent constraints on the heavy Higgs states as the $b\bar{b}$ production would be overwhelmed by a huge QCD background. However, the current bound and exclusion limit of $\tau\tau$ channel are generally based on predictions from generic two Higgs doublet model or some particular SUSY benchmarks [10]. As well known, the fit to 126 GeV Higgs mass and signal excesses leads to light SUSY sparticles, for instance superpartners of top quark and tau lepton. Given light SUSY spectrum, the heavy neutral Higgses decay would change dramatically and result into altered exclusion limit of $\tau\tau$ channel [11]. The SUSY products effect in the heavy Higgs decay would also open rich LHC phenomenology. This paper aims to examine the current status of decoupling scenario and future perspectives for heavy Higgses decay and production. We highlight the complex pattern of heavy Higgses decay, in particular for small $\tan\beta$ region, taking into account the updated Higgs search bounds and latest flavor measurements. We perform the extrapolation of $\tau\tau$ mode to the center-of-mass energy of 14 TeV with high luminosities at the LHC.

The rest of the paper is organized as follows. In Sec. II, we present the parameter choices relevant for Higgs observation in our scan. We also present the scanning results with subject to the constraints from the searches of Higgs and sparticles and flavor measurements. We also highlight the exotic patterns of heavy Higgs decay and extrapolate the $\tau\tau$ decay mode in Sec. III. We summarize our results in Sec. IV.

II. SUSY PARAMETER REGION AND EXPERIMENTAL BOUNDS

To figure out the impact of experimental data on SUSY, it is crucial to scan the parameters relevant for the current Higgs observation and flavor measurements and extract the surviving space. We follow the procedure in Ref. [4] to explore the consistent parameter space. To perform a comprehensive scan over the MSSM parameter space, besides the parameters adopted in Ref. [4], we take into account the stau sector in the scan

$$1 < \tan\beta < 55, \quad 50 \text{ GeV} < M_A < 1000 \text{ GeV}, \quad 100 \text{ GeV} < \mu < 2000 \text{ GeV}, \quad (1)$$

$$100 \text{ GeV} < M_{\tilde{t}_R}, M_{\tilde{Q}_3} < 2000 \text{ GeV}, \quad -4000 \text{ GeV} < A_t < 4000 \text{ GeV}, \quad (2)$$

$$100 \text{ GeV} < M_{\tilde{\tau}_R}, M_{\tilde{L}_3} < 2000 \text{ GeV}, \quad -4000 \text{ GeV} < A_\tau < 4000 \text{ GeV}, \quad (3)$$

$$100 \text{ GeV} < M_2 < 2000 \text{ GeV}. \quad (4)$$

In addition, we focus on the reduced high M_A range in order to study the decoupling region:

$$300 \text{ GeV} < M_A < 1000 \text{ GeV}. \quad (5)$$

The $U(1)$ gaugino mass M_1 , however, is unconstrained in the MSSM since Bino does not contribute much to either the Higgs sector, or the flavor observables. Moreover, as indicated by the measurement of dark matter relic density, the dark matter candidate in the MSSM is more likely to be a Bino-like neutralino with a mass heavier than 30 GeV [12, 13]. We thus prefer the Bino neutralino as the lightest supersymmetric particle (LSP) and take $m_{\tilde{\chi}_1^0} \approx M_1 = 90 \text{ GeV}$ for illustration, unless stated otherwise. Other SUSY soft masses, which are less relevant to our consideration, are all fixed to be 3 TeV.

A. Constraints from the Higgs Searches and b Rare Decays

We perform our scan by using the FeynHiggs 2.9.5 package [14–17] to calculate the Higgs masses, SUSY spectrum, couplings and Higgs decay/production rates. HiggsBound 4.0.0 [18] is used to impose the exclusion constraints from LEP2 [19], the Tevatron [20] and the LHC. We further require that the light CP-even Higgs boson is SM-like and satisfies the following properties

$$h^0 \text{ in the mass range of } 124 \text{ GeV} - 128 \text{ GeV}, \quad (6)$$

$$\sigma \times \text{BR}(gg \rightarrow h^0 \rightarrow \gamma\gamma)_{\text{MSSM}} \geq 80\%(\sigma \times \text{BR})_{\text{SM}}, \quad (7)$$

$$\sigma \times \text{BR}(gg \rightarrow h^0 \rightarrow WW/ZZ)_{\text{MSSM}} \geq 40\%(\sigma \times \text{BR})_{\text{SM}}. \quad (8)$$

The experimental flavor measurements considered here include $b \rightarrow s\gamma$ [21] and the LHCb report on $B_s \rightarrow \mu^+\mu^-$ [22]. In our study, we use the following experimental limits

$$\text{BR}(B_s \rightarrow X_s\gamma)_{\text{exp}} = (3.43 \pm 0.21) \times 10^{-4}, \quad \text{BR}(B_s \rightarrow \mu^+\mu^-)_{\text{exp}} = (2.9_{-1.0}^{+1.1}) \times 10^{-9}, \quad (9)$$

which are consistent with SM predictions [23–25]

$$\text{BR}(B_s \rightarrow X_s\gamma)_{\text{SM}} = (3.15 \pm 0.23) \times 10^{-4}, \quad \text{BR}(B_s \rightarrow \mu^+\mu^-)_{\text{SM}} = (3.23 \pm 0.27) \times 10^{-9} \quad (10)$$

BABAR also reported improved measurements of $B \rightarrow D\tau\nu_\tau$ which indicates a deviation from the SM expectation. We take the observed excess as an upper limit [26]

$$\frac{\text{BR}(B \rightarrow D\tau\nu_\tau)}{\text{BR}(B \rightarrow D\ell\nu_\ell)} < 0.44, \quad \frac{\text{BR}(B \rightarrow D\tau\nu_\tau)_{\text{SM}}}{\text{BR}(B \rightarrow D\ell\nu_\ell)_{\text{SM}}} = 0.297 \pm 0.017. \quad (11)$$

In our numerical study, we use SuperIso 3.3 [27] to evaluate the above flavor observables.

B. Results for Allowed Region

We generate sufficient random data samples and pass them through the above constraints. Taking into account both the Higgs search results and the flavor constraints, we first show the surviving points in Fig. 1 in the $\tan\beta - m_A$ plane. One can see that the measured Higgs mass window and current Higgs search data push the lower limit of m_A to 400 GeV. Further b rare decay constraints allow the whole region of $m_A > 400$ GeV and $5 < \tan\beta < 40$. However, due to the enhancement of MSSM contributions to $B_s \rightarrow \mu^+\mu^-$ by $\tan^6\beta$ and reduction by $1/m_A^4$, the large $\tan\beta$ and small m_A regime is highly constrained by b rare decays. Note that although some points have $\tan\beta \gtrsim 45$, more data probing for heavy Higgs regime in near future would immediately restrict $m_A > 800$ GeV with large $\tan\beta$. In the following we examine the surviving region favored by Higgs observation and flavor constraints.

In the MSSM, as is well-known, the loop correction of the lightest MSSM Higgs mass is dominated by the stop sector and can raise m_{h^0} to the observed value of Higgs boson mass. The leading stop loop correction is given by [28]

$$\epsilon = \frac{3m_t^4}{2\pi^2 v^2 \sin^2\beta} \left[\ln\left(\frac{M_S^2}{m_t^2}\right) + \frac{X_t^2}{M_S^2} \left(1 - \frac{X_t^2}{12M_S^2}\right) \right], \quad (12)$$

where $X_t = A_t - \mu \cot\beta$ and $M_S = \sqrt{m_{\tilde{t}_1} m_{\tilde{t}_2}}$. Thus, as the measured Higgs mass is relatively heavier than tree level MSSM Higgs, the stop masses and stop mixing parameter, X_t , are strongly related to the Higgs mass in the MSSM. Satisfying the Higgs mass constraint, the stop masses are approximately given by [29]

$$m_{\tilde{t}_1}^2 \simeq m_{\tilde{Q}_3}^2 + m_t^2 \left(1 - \frac{X_t^2}{m_{\tilde{t}_R}^2}\right), \quad m_{\tilde{t}_2}^2 \simeq m_{\tilde{t}_R}^2 + m_t^2 \left(1 + \frac{X_t^2}{m_{\tilde{t}_R}^2}\right), \quad \text{for } |X_t| \simeq m_{\tilde{t}_R} \gg m_{\tilde{Q}_3}, \quad (13)$$

with the switch of $m_{\tilde{Q}_3} \leftrightarrow m_{\tilde{t}_R}$ for $|X_t| \simeq m_{\tilde{Q}_3} \gg m_{\tilde{t}_R}$, unless both stops are very heavy. The light stop is thus mostly left-handed (right-handed) and its mass is governed by $m_{\tilde{Q}_3}$ ($m_{\tilde{t}_R}$) for $m_{\tilde{t}_R} \gg m_{\tilde{Q}_3}$ ($m_{\tilde{Q}_3} \gg m_{\tilde{t}_R}$). The physical stop masses are shown in Fig. 2 (a). As seen from the stop mixing effect in Fig. 2 (b) in the plane of $X_t/\sqrt{m_{\tilde{Q}_3} m_{\tilde{t}_R}}$ vs. $m_{\tilde{t}_1}$, the ranges of $X_t, m_{\tilde{Q}_3}, m_{\tilde{t}_R}$ sit nearly maximal stop mixing for light stops. Note that the values of light sbottom and sneutrino mass are determined by $m_{\tilde{Q}_3}$ and $m_{\tilde{L}_3}$, respectively, and thus mostly \tilde{b}_L and $\tilde{\nu}_{\tau L}$.

As well discussed before, there are two main mechanisms leading to a simultaneous enhancement of the diphoton production rate in the MSSM [30]. Firstly, the largest partial contribution to the total width of SM-like Higgs decay, namely $\Gamma(h^0 \rightarrow b\bar{b})$, would decrease if the bottom

Yukawa is enhanced. As a result, the total decay width of h^0 will be reduced and thus the $\gamma\gamma$ rate gets enhancement. Figs. 3 (a) and (b) show the allowed parameter space relevant for the SM-like Higgs production: (a) μ versus M_2 and (b) A_t versus $m_{\tilde{Q}_3}$. The current Higgs bounds strongly favor relatively large μ and positive A_t with $|A_t| \gtrsim 2$ TeV. This is because large positive product μA_t leads to a large positive radiative correction to bottom Yukawa which is needed to suppress $\Gamma(h^0 \rightarrow b\bar{b})$ so as to enhance $\sigma(gg \rightarrow h^0 \rightarrow \gamma\gamma)$ [4, 30].

The second mechanism is due to the effect of SUSY particles in the direct enhancement of the $\Gamma(h^0 \rightarrow gg/\gamma\gamma)$, for instance light stop and stau [31]. The stop loop contributions to the gg and $\gamma\gamma$ amplitudes are approximately proportional to [29, 32]

$$\pm \frac{m_t^2}{m_{\tilde{t}_1}^2 m_{\tilde{t}_2}^2} (m_{\tilde{t}_1}^2 + m_{\tilde{t}_2}^2 - X_t^2). \quad (14)$$

Hence, we show the stop effect in Higgs production described in Eq. (14) in Fig. 3 (c) in the plane of $(m_{\tilde{t}_1}^2 + m_{\tilde{t}_2}^2 - X_t^2)/10^4$ GeV versus $m_{\tilde{t}_1}$. For light stop, as one can see, the enhanced contribution of stop in the $\Gamma(h^0 \rightarrow \gamma\gamma)$ dominates over the reduction in the gluon fusion production such that for $gg \rightarrow h^0 \rightarrow \gamma\gamma$ rate being above 0.8 of the SM value. Moreover, an enhancement of $\Gamma(h^0 \rightarrow \gamma\gamma)/\Gamma(h^0 \rightarrow \gamma\gamma)_{SM}$ as large as a factor of 1.25 is possible as a result of light stau effect in the loop, as seen in Fig. 3 (d).

C. Discussion of SUSY Sparticle Searches

Additional constraints come from direct sparticle searches, for instance stop and sbottom. In principle, the stop and sbottom mass limit drops lower for small mass difference between the stop/sbottom and the Bino LSP. One can always tune the free Bino mass to be large enough to give soft decay products and thus evade the stop/sbottom search limits. Recently, ATLAS reported that light stops with $m_{\tilde{t}_1} \lesssim 200$ GeV and any kinematically allowed neutralino LSP mass are essentially excluded if $BR(\tilde{t}_1 \rightarrow c\tilde{\chi}_1^0) = 100\%$ [33]. However, this bound could be weakened if other decay mode with lighter sparticle, such as $\tilde{t}_1 \rightarrow \tilde{\tau}_1 \nu_\tau b$, overwhelms $\tilde{t}_1 \rightarrow c\tilde{\chi}_1^0$ as pointed out in Ref. [29]. Also, if Bino mass is not that large and $m_{\tilde{t}_1} - m_{\tilde{\chi}_1^0} > m_W + m_b$ (m_t), the main decay mode is given by $\tilde{t}_1 \rightarrow bW^+ \tilde{\chi}_1^0$ ($t\tilde{\chi}_1^0$). We then have freedom for Bino mass to survive light stop, given the gap between stop bound and kinematic limit.

ATLAS also released that any sbottom with mass less than 650 GeV is not allowed if $m_{\tilde{\chi}_1^0} < 100$ GeV and $BR(\tilde{b}_1 \rightarrow b\tilde{\chi}_1^0) = 100\%$ [34]. For small values of $m_{\tilde{Q}_3}$, we have light left-handed

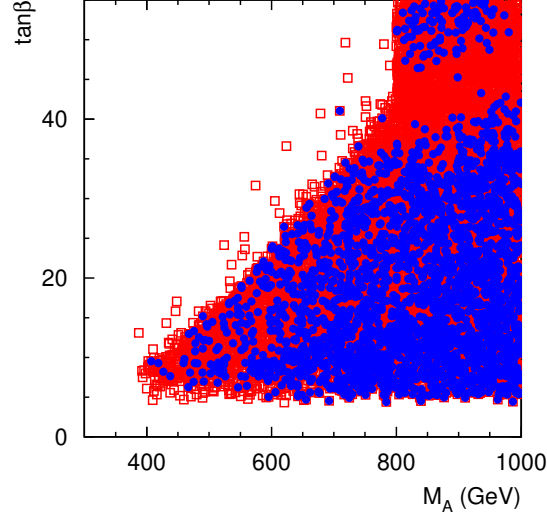


FIG. 1: $\tan \beta$ vs. m_A for surviving points satisfying bounds from LEP2, Tevatron, LHC and $m_{h^0} = 126 \pm 2$ GeV (red open square), and further including b rare decay constraints (blue filled circle). The following figures are all for points passing all constraints considered here.

sbottom in the spectrum as $m_{\tilde{b}_1} \sim m_{\tilde{Q}_3}$. Thus, this case tends to be in conflict with the above limit if $m_{\tilde{b}_1} - m_{\tilde{\chi}_1^0} \gtrsim 20$ GeV or $m_{\tilde{\chi}_1^0} < 100$ GeV. However, if Wino neutralino stays between sbottom and Bino LSP, the left-handed sbottom prefers to decay to it with $BR(\tilde{b}_1 \rightarrow b\tilde{\chi}_2^0)$ being typically around 80%-90% [8], even though relatively suppressed by the available phase space. With the further decay of $\tilde{\chi}_2^0$ into $h^{0(*)}\tilde{\chi}_1^0$ or $Z^{(*)}\tilde{\chi}_1^0$, these longer decay chains give soft decay products and small missing energy undetected in the detector. As a result, the current sbottom search would not highly restrict the small $m_{\tilde{Q}_3}$ case.

In addition, CMS put the lower limit on the $m_{\tilde{\chi}_1^\pm, \tilde{\chi}_2^0}$ to 330 GeV under the assumption of $m_{\tilde{\chi}_2^0} - m_{\tilde{\chi}_1^0} > m_Z$ and $BR(\tilde{\chi}_2^0 \rightarrow Z\tilde{\chi}_1^0) = BR(\tilde{\chi}_1^\pm \rightarrow W^\pm\tilde{\chi}_1^0) = 100\%$ [35]. This limit would not directly constrain the spectrum with small mass difference $m_{\tilde{\chi}_2^0} - m_{\tilde{\chi}_1^0}$ as well as possible suppression of chargino/neutralino decays.

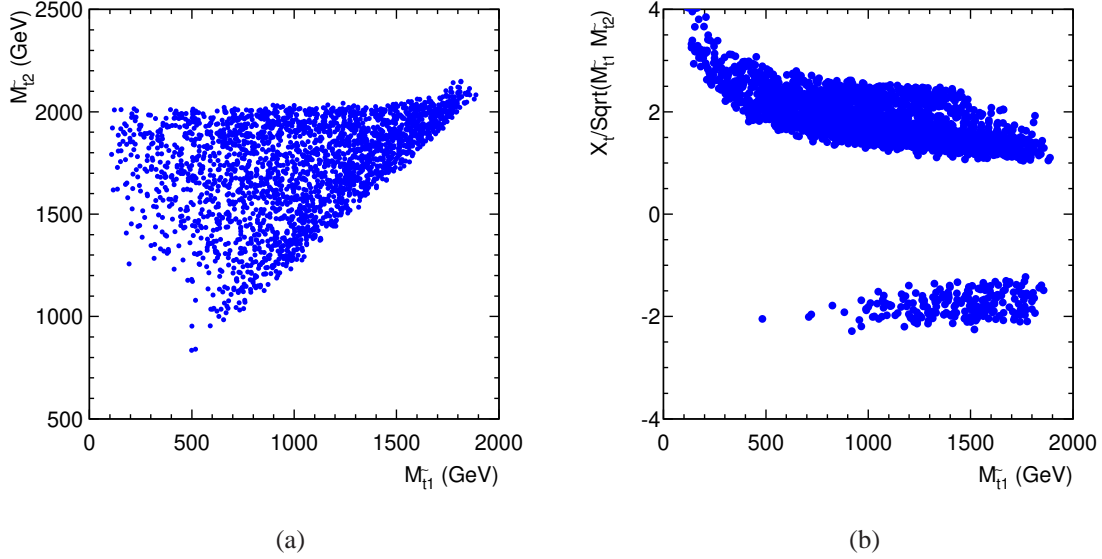


FIG. 2: (a) $m_{\tilde{t}_2}$ vs. $m_{\tilde{t}_1}$ and (b) $X_t / \sqrt{m_{\tilde{t}_1} m_{\tilde{t}_2}}$ vs. $m_{\tilde{t}_1}$.

III. HEAVY HIGGS DECAY AND SEARCH SENSITIVITY

A. Heavy Higgs Decay

In the decoupling limit, the heavy non SM-like Higgses H^0 , A^0 and H^\pm have rich decay modes, especially in the small $\tan\beta$ regime. Figs. 4 and 5 show the branching ratios of heavy neutral Higgs bosons decay into fermion pairs. In this limit, the H^0/A^0 coupling to the top quarks is suppressed by $1/\tan\beta$, while the couplings to bottom quarks and tau leptons are enhanced by $\tan\beta$. As seen in Fig. 4, a majority of points have $BR(H^0/A^0 \rightarrow b\bar{b}) \sim 80\%$ and $BR(H^0/A^0 \rightarrow \tau^+\tau^-) \sim 20\%$. However, for exceptional significant points in Figs. 4 and 5, the $H^0/A^0 \rightarrow t\bar{t}$ mode could be dominant for $\tan\beta \lesssim 10$ in particular.

Fig. 3 (a) shows that small values of μ , M_2 are allowed. We thus expect kinematically occurred heavy Higgs decay into pairs of chargino and neutralino. The MSSM Higgs bosons mainly couple to mixtures of higgsino and gaugino components [3]. Therefore, for $\mu \gg M_{1,2}$ or $\mu \ll M_{1,2}$, the decays of the heavy Higgs bosons into pairs of pure gaugino or higgsino are strongly suppressed. The mixed decay $H^0/A^0 \rightarrow \tilde{\chi}_1^\pm \tilde{\chi}_2^\mp, \tilde{\chi}_{1,2}^0 \tilde{\chi}_{3,4}^0$ will then have significant branching fractions. For $\mu \sim M_2$, on the other hand, all the heavy Higgses have comparable decay rates into

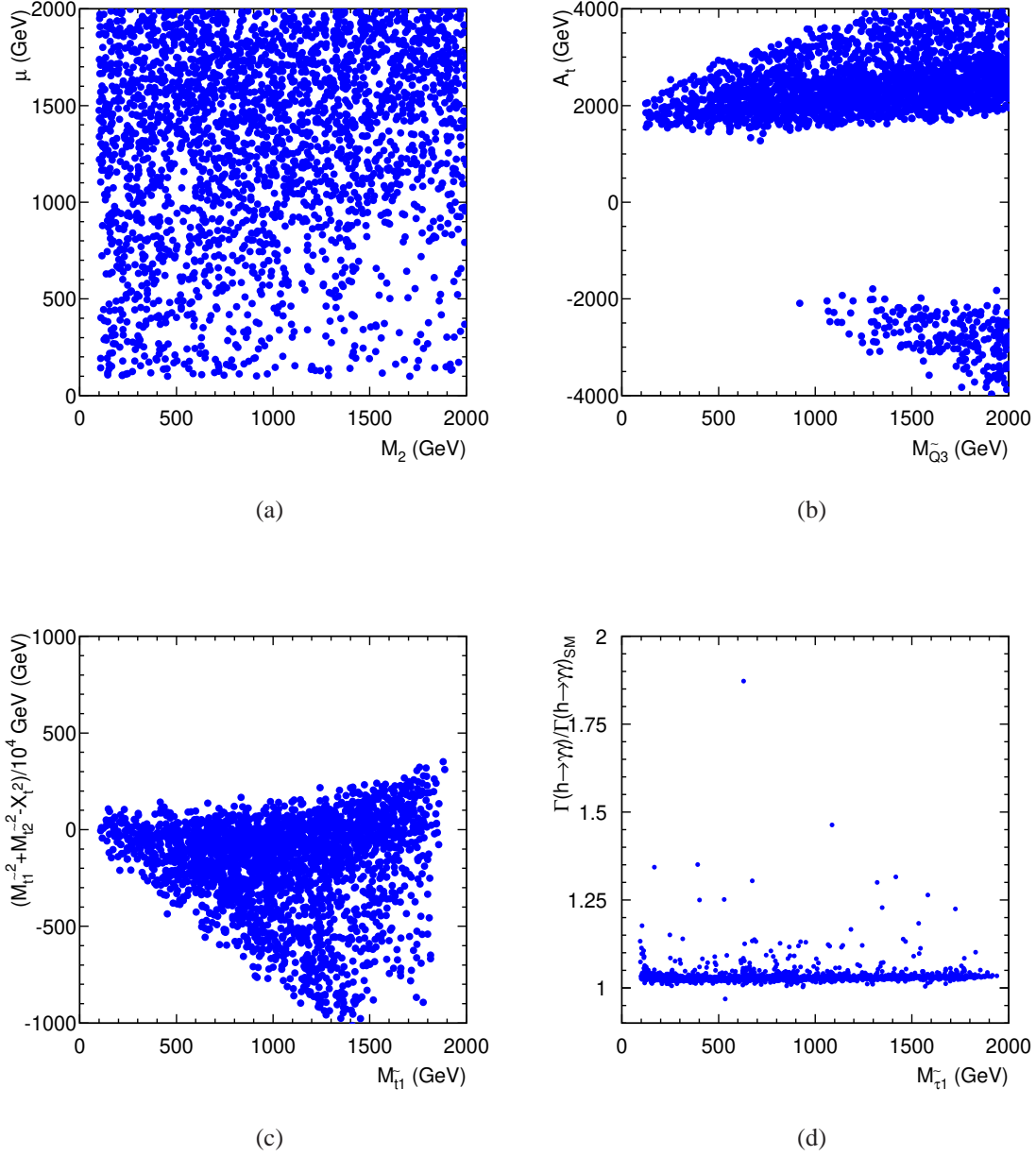


FIG. 3: (a) μ versus M_2 , (b) A_t versus $m_{\tilde{Q}_3}$, (c) $(m_{t_1}^2 + m_{t_2}^2 - X_t^2)/10^4$ GeV versus $m_{\tilde{t}_1}$ and (d) $\Gamma(h^0 \rightarrow \gamma\gamma)/\Gamma(h^0 \rightarrow \gamma\gamma)_{SM}$ versus $m_{\tilde{t}_1}$.

chargino/neutralino. We show the $BR(H^0/A^0 \rightarrow \tilde{\chi}_i^\pm \tilde{\chi}_j^\mp)$ and $BR(H^0/A^0 \rightarrow \tilde{\chi}_i^0 \tilde{\chi}_j^0)$ in Figs. 6, 7 and 8. One can see that the branching ratio of chargino and neutralino decay mode can reach at most 40% and 20%, respectively. In particular, the invisible decay mode of heavy higgs, namely $H^0/A^0 \rightarrow \tilde{\chi}_1^0 \tilde{\chi}_1^0$, relies on the arbitrary Bino LSP mass and has important implication for the dark

matter candidate search at the LHC. We display $BR(H^0/A^0 \rightarrow \tilde{\chi}_1^0 \tilde{\chi}_1^0)$ as a function of $m_{\tilde{\chi}_1^0}$ in Fig. 9. The $BR(H^0/A^0 \rightarrow \tilde{\chi}_1^0 \tilde{\chi}_1^0)$ increases with increasing Bino LSP mass and is between 10%-15% (20%) for $30 < m_{\tilde{\chi}_1^0} < 100$ GeV. This invisible decay mode can be tested through mono-b jet signature in $gb \rightarrow bH^0/A^0$ production.

Indicated by the fit to Higgs mass and signals, light sfermions also play important role in the heavy Higgs decay. In the decoupling limit, the heavy neutral Higgses couplings to sfermion current eigenstates are given by [3]

$$C_{H^0 \tilde{f} \tilde{f}} = \begin{pmatrix} (I_f^{3L} - Q_f s_W^2) m_Z^2 \sin 2\beta + m_f^2 r_1^f & \frac{1}{2} m_f (A_f r_1^f + \mu r_2^f) \\ \frac{1}{2} m_f (A_f r_1^f + \mu r_2^f) & Q_f s_W^2 m_Z^2 \sin 2\beta + m_f^2 r_1^f \end{pmatrix}, \quad (15)$$

$$C_{A^0 \tilde{f} \tilde{f}} = \begin{pmatrix} 0 & -\frac{1}{2} m_f (A_f (\tan \beta)^{-2I_3^f} + \mu) \\ \frac{1}{2} m_f (A_f (\tan \beta)^{-2I_3^f} + \mu) & 0 \end{pmatrix}, \quad (16)$$

where $r_1^u = -\cot \beta$, $r_1^d = r_1^l = -\tan \beta$, $r_2^u = -1$ and $r_2^d = r_2^l = 1$. For CP-even Higgs H^0 , these couplings contain term proportional to m_f^2 and thus get enhanced for the third generation sfermions. The CP-odd Higgs A^0 only couples to $\tilde{f}_1 \tilde{f}_2$ mixtures with couplings $\propto m_f$. The stop decay mode for A^0 is then forbidden as at least one stop has to be very heavy to accommodate SM-like Higgs mass. Figs. 10 (a) and (b) show that the branching fraction of heavy Higgses decay into sfermions can be as large as 80% for $H^0 \rightarrow \tilde{t}_1 \tilde{t}_1^*$ and 60% for $H^0/A^0 \rightarrow \tilde{\tau}_1 \tilde{\tau}_2^* + \tilde{\tau}_1^* \tilde{\tau}_2$. Moreover, with increasing $|A_\tau|$, both H^0 and A^0 have increasing branching ratio of $\tilde{\tau}_1 \tilde{\tau}_2^* + \tilde{\tau}_1^* \tilde{\tau}_2$ decay mode [29], as seen from Figs. 10 (c) and (d). In Fig. 11 we display the dependence of heavy Higgs decay into light sfermions on SUSY soft masses. The decay $H^0 \rightarrow \tilde{t}_1 \tilde{t}_1^*$ is dominant for either $m_{\tilde{Q}_3} < 500$ GeV, $m_{\tilde{t}_R} > 1.2$ TeV or $m_{\tilde{Q}_3} > 1.2$ TeV, $m_{\tilde{t}_R} < 500$ GeV with only one light stop. While $H^0 \rightarrow \tilde{\tau}_1 \tilde{\tau}_2^* + \tilde{\tau}_1^* \tilde{\tau}_2$ could be dominant for $m_{\tilde{L}_3}, m_{\tilde{\tau}_R} < 800$ GeV with two light staus.

The decays $H^0 \rightarrow h^0 h^0$ and $A^0 \rightarrow h^0 Z$ are known to complement heavy Higgs searches at low values of $\tan \beta$ and intermediate M_A masses [9, 36]. In the decoupling limit with $M_A > 400$ GeV constrained by current Higgs searches, the corresponding partial decay widths are suppressed by $1/m_{H^0}$ and coupling $\cos^2(\beta - \alpha) \ll 1$, respectively. Their branching fractions are thus decreasing quickly with at most 10% for $H^0 \rightarrow h^0 h^0$ and 1% for $A^0 \rightarrow h^0 Z$ as seen in Fig. 12.

Finally, we show the branching fraction of charged Higgs decay in Fig. 13. A majority of points give $BR(H^+ \rightarrow t\bar{b}) \sim 80\%$ and $BR(H^+ \rightarrow \tau^+ \nu_\tau) \sim 20\%$. The branching ratio of charged Higgs decay to light neutralino plus chargino and sfermions can be as large as 40% and 60%, respectively.

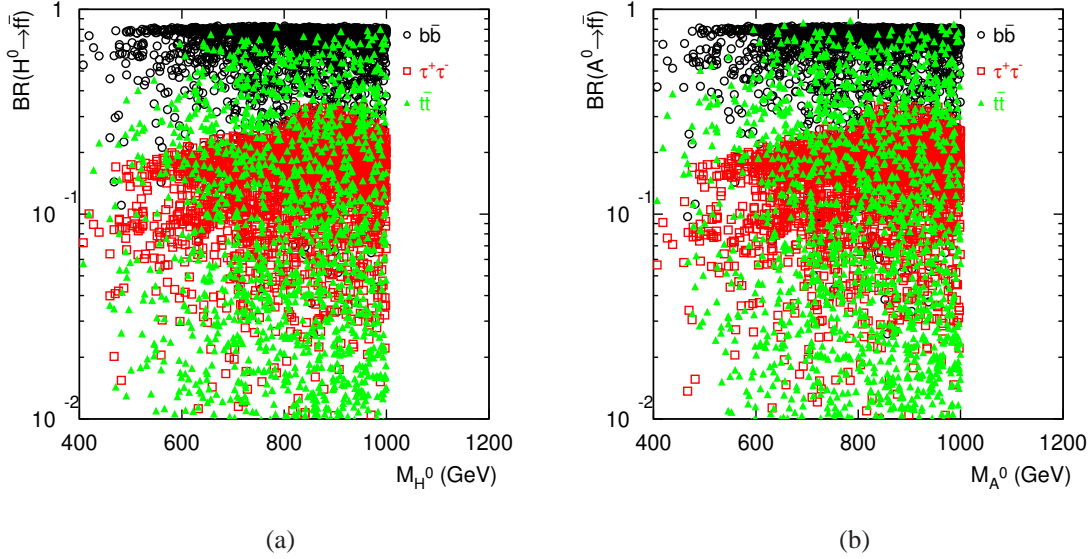


FIG. 4: (a) $BR(H^0 \rightarrow f\bar{f})$ vs. m_{H^0} and (b) $BR(A^0 \rightarrow f\bar{f})$ vs. m_{A^0} .

B. Future Heavy Higgs Search Sensitivity

As one can see from previous subsection, SUSY effects could vary the $\tau\tau$ mode of heavy Higgs decay significantly. One has to consider the variation of $\tau\tau$ exclusion limit given various SUSY decay products, for the small values of $\tan\beta$ in particular. We now improve measurement potential for the search of heavy MSSM Higgs decay into $\tau^+\tau^-$. Assuming the signal and background events go up by the same factor when the energy enhanced, we simply scale the signal sensitivity with $\sqrt{\sigma_{signal} \times L}$ based on the expected upper limit on the $\tau\tau$ channel [10], where $\sigma_{signal} = \sigma(gg, b\bar{b} \rightarrow H^0, A^0 \rightarrow \tau^+\tau^-)$ at 14 TeV LHC and L is the integrated luminosity. The extrapolation of excluded region for $\tau\tau$ mode at 14 TeV LHC is shown in Fig. 14 with $L = 300 \text{ fb}^{-1}$ and 3000 fb^{-1} . One can see that, in the plane of $\tan\beta - M_A$ with $M_A < 800 \text{ GeV}$, the $\tau\tau$ mode can only essentially exclude regime with $\tan\beta > 20$ for $L = 300 \text{ fb}^{-1}$ and $\tan\beta > 15$ for $L = 3000 \text{ fb}^{-1}$.

IV. CONCLUSIONS

The decoupling limit in the MSSM Higgs sector is the most likely scenario in light of the Higgs discovery. This scenario is further constrained by MSSM Higgs search bounds and fla-

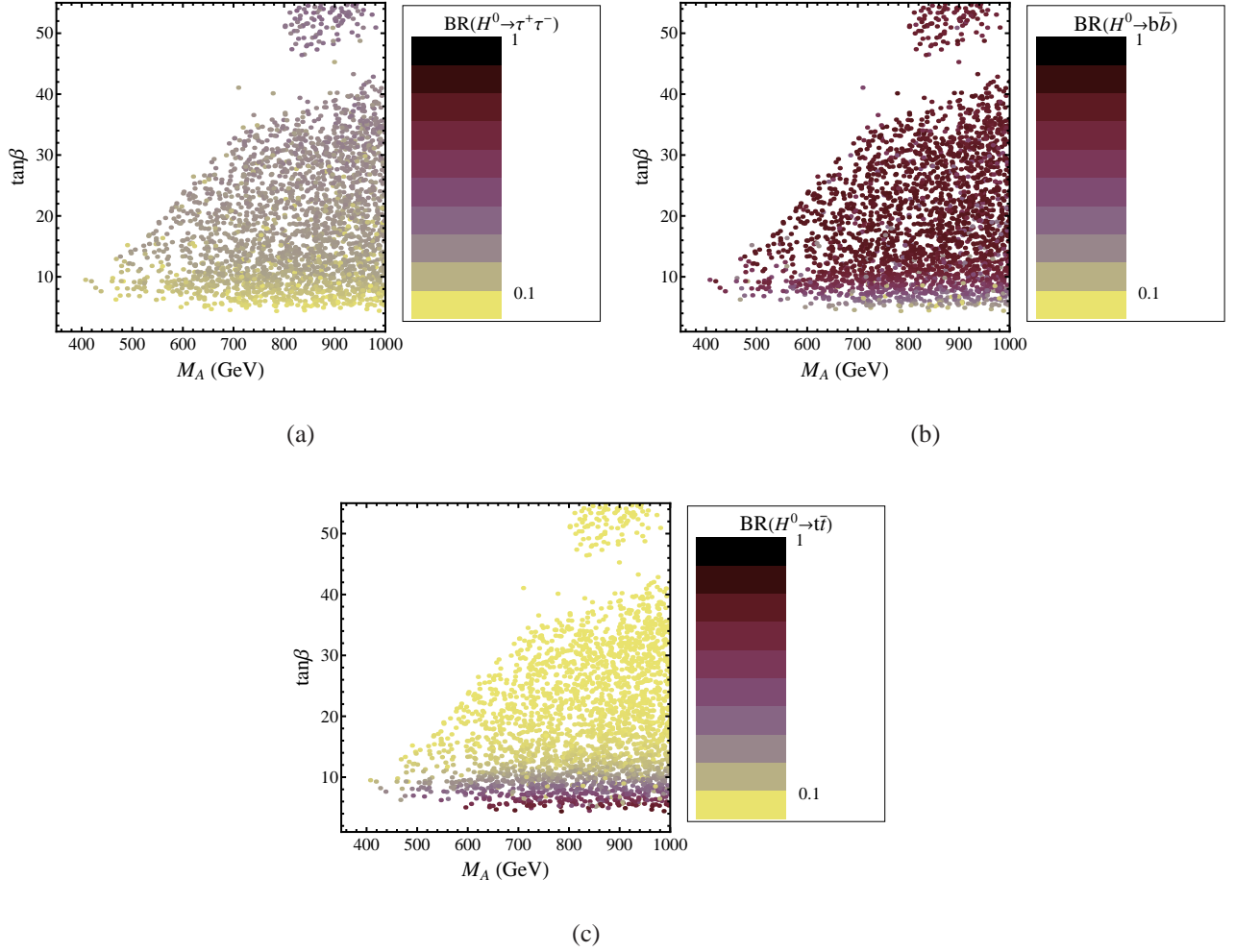


FIG. 5: $BR(H^0 \rightarrow f\bar{f})$ in the plane of $\tan\beta$ vs. M_A , for (a) $f = \tau$, (b) $f = b$ and (c) $f = t$. The color scale gives the branching fraction of $H^0 \rightarrow f\bar{f}$ decay.

vor measurements. We performed a comprehensive scan of MSSM parameter space and updated the constraints on the decoupling MSSM Higgs sector in terms of 8 TeV data. The light SUSY spectrum in charge of SM-like Higgs mass and signal excesses was discussed. We highlighted the effect of light SUSY spectrum in the heavy neutral Higgs decay in the decoupling limit. We found that the measured Higgs mass window and current Higgs search data push m_A to at least 400 GeV. Further b rare decays do not put more stringent constraints on the surviving region. The chargino and neutralino decay mode can reach at most 40% and 20% branching ratio, respectively. In particular, the invisible decay $BR(H^0(A^0) \rightarrow \tilde{\chi}_1^0 \tilde{\chi}_1^0)$ increases with increasing Bino LSP mass and sits between 10%-15% (20%) for $30 < m_{\tilde{\chi}_1^0} < 100$ GeV. The branching fraction of dom-

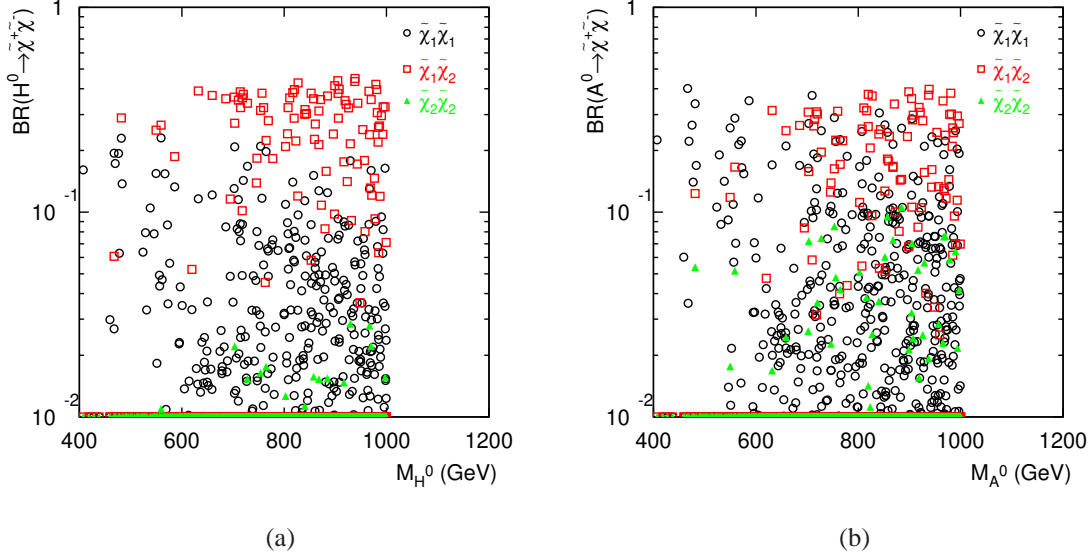


FIG. 6: (a) $BR(H^0 \rightarrow \tilde{\chi}_i^\pm \tilde{\chi}_j^\mp)$ vs. m_{H^0} and (b) $BR(A^0 \rightarrow \tilde{\chi}_i^\pm \tilde{\chi}_j^\mp)$ vs. m_{A^0} .

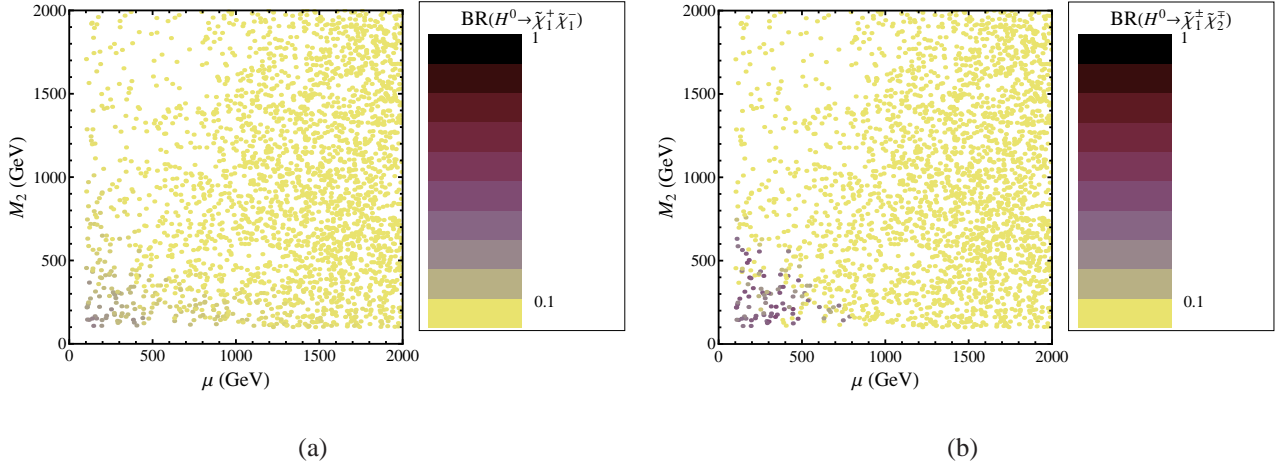


FIG. 7: $BR(H^0 \rightarrow \tilde{\chi}_i^\pm \tilde{\chi}_j^\mp)$ in the plane of M_2 vs. μ , for (a) $i = j = 1$ and (b) $i = 1, j = 2$. The color scale gives the branching fraction of $H^0 \rightarrow \tilde{\chi}_i^\pm \tilde{\chi}_j^\mp$ decay.

inant heavy Higgses decay into sfermions can be as large as 80% for $H^0 \rightarrow \tilde{t}_1 \tilde{t}_1^*$ and 60% for $H^0/A^0 \rightarrow \tilde{\tau}_1 \tilde{\tau}_2^* + \tilde{\tau}_1^* \tilde{\tau}_2$. $H^0 \rightarrow h^0 h^0$ and $A^0 \rightarrow h^0 Z$ have the branching fraction less than 10% and 1%, respectively, for $m_A > 400$ GeV. The branching ratio of charged Higgs decay to neutralino

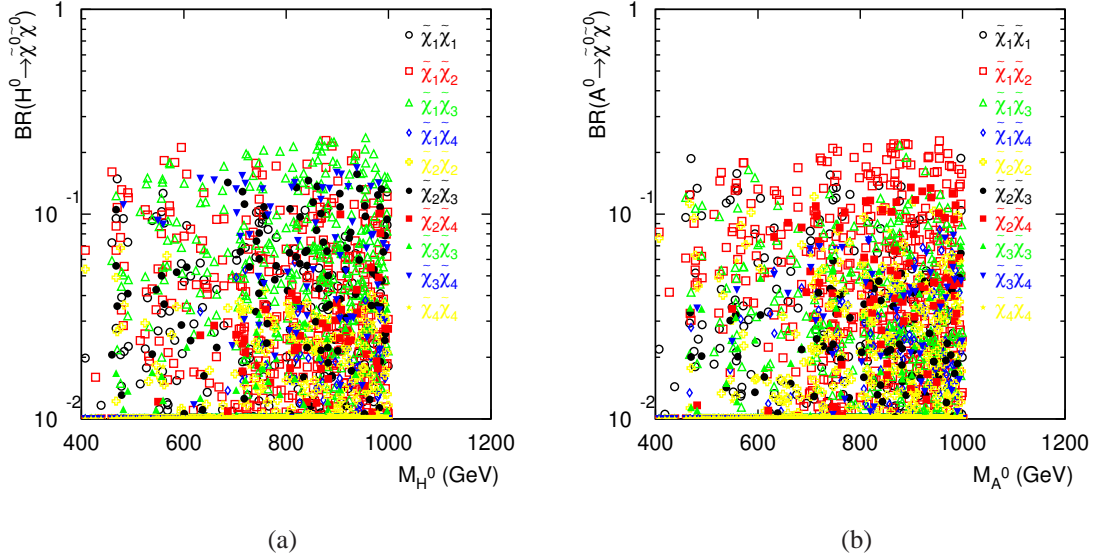


FIG. 8: (a) $BR(H^0 \rightarrow \tilde{\chi}_i^0 \tilde{\chi}_j^0)$ vs. m_{H^0} and (b) $BR(A^0 \rightarrow \tilde{\chi}_i^0 \tilde{\chi}_j^0)$ vs. m_{A^0} .

plus chargino and sfermions can be as large as 40% and 60%, respectively. Moreover, these dominant SUSY products alter the normal heavy Higgs decay modes dramatically, in particular for small $\tan \beta$ region. We extrapolated the exclusion limit of leading MSSM Higgs search channel, namely $gg, b\bar{b} \rightarrow H^0, A^0 \rightarrow \tau^+ \tau^-$, to center-of-mass energy of 14 TeV with high luminosities at the LHC based on surviving region and exceptions of dominant SUSY decay channels. It turns out that the $\tau\tau$ mode can essentially exclude regime with $\tan \beta > 20$ for $L = 300 \text{ fb}^{-1}$ and $\tan \beta > 15$ for $L = 3000 \text{ fb}^{-1}$.

Acknowledgment

We would like to thank Marcela Carena and Ian Lewis for useful discussions. This work was supported in part by the Australian Research Council.

-
- [1] G. Aad *et al.* [ATLAS Collaboration], Phys. Lett. B **716**, 1 (2012) [arXiv:1207.7214 [hep-ex]]; S. Chatrchyan *et al.* [CMS Collaboration], Phys. Lett. B **716**, 30 (2012) [arXiv:1207.7235 [hep-ex]].

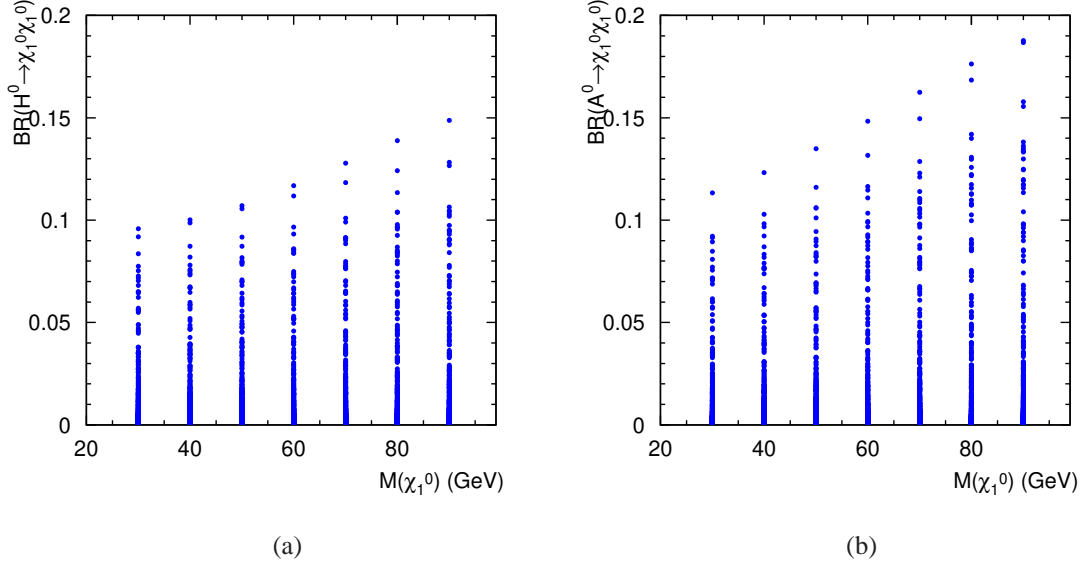


FIG. 9: (a) $BR(H^0 \rightarrow \tilde{\chi}_1^0 \tilde{\chi}_1^0)$ vs. $m_{\tilde{\chi}_1^0}$ and (b) $BR(A^0 \rightarrow \tilde{\chi}_1^0 \tilde{\chi}_1^0)$ vs. $m_{\tilde{\chi}_1^0}$.

- [2] J. F. Gunion, H. E. Haber, G. L. Kane and S. Dawson, *Front. Phys.* **80**, 1 (2000); J. F. Gunion and H. E. Haber, *Nucl. Phys. B* **272**, 1 (1986) [Erratum-ibid. B **402**, 567 (1993)].
- [3] A. Djouadi, *Phys. Rept.* **459**, 1 (2008) [hep-ph/0503173].
- [4] N. D. Christensen, T. Han and S. Su, *Phys. Rev. D* **85**, 115018 (2012) [arXiv:1203.3207 [hep-ph]].
- [5] H. E. Haber, hep-ph/9501320.
- [6] H. E. Haber, hep-ph/9505240.
- [7] N. D. Christensen, T. Han and T. Li, *Phys. Rev. D* **86**, 074003 (2012) [arXiv:1206.5816 [hep-ph]].
- [8] T. Han, T. Li, S. Su and L. -T. Wang, arXiv:1306.3229 [hep-ph].
- [9] A. Arbey, M. Battaglia and F. Mahmoudi, *Phys. Rev. D* **88**, 015007 (2013) [arXiv:1303.7450 [hep-ph]].
- [10] S. Chatrchyan *et al.* [CMS Collaboration], CMS PAS HIG-12-050.
- [11] I. M. Lewis, arXiv:1308.1742 [hep-ph].
- [12] M. Carena, S. Gori, N. R. Shah, C. E. M. Wagner and L. -T. Wang, *JHEP* **1207**, 175 (2012) [arXiv:1205.5842 [hep-ph]].
- [13] T. Han, Z. Liu and A. Natarajan, arXiv:1303.3040 [hep-ph].
- [14] G. Degrandi, S. Heinemeyer, W. Hollik, P. Slavich and G. Weiglein, *Eur. Phys. J. C* **28**, 133 (2003)

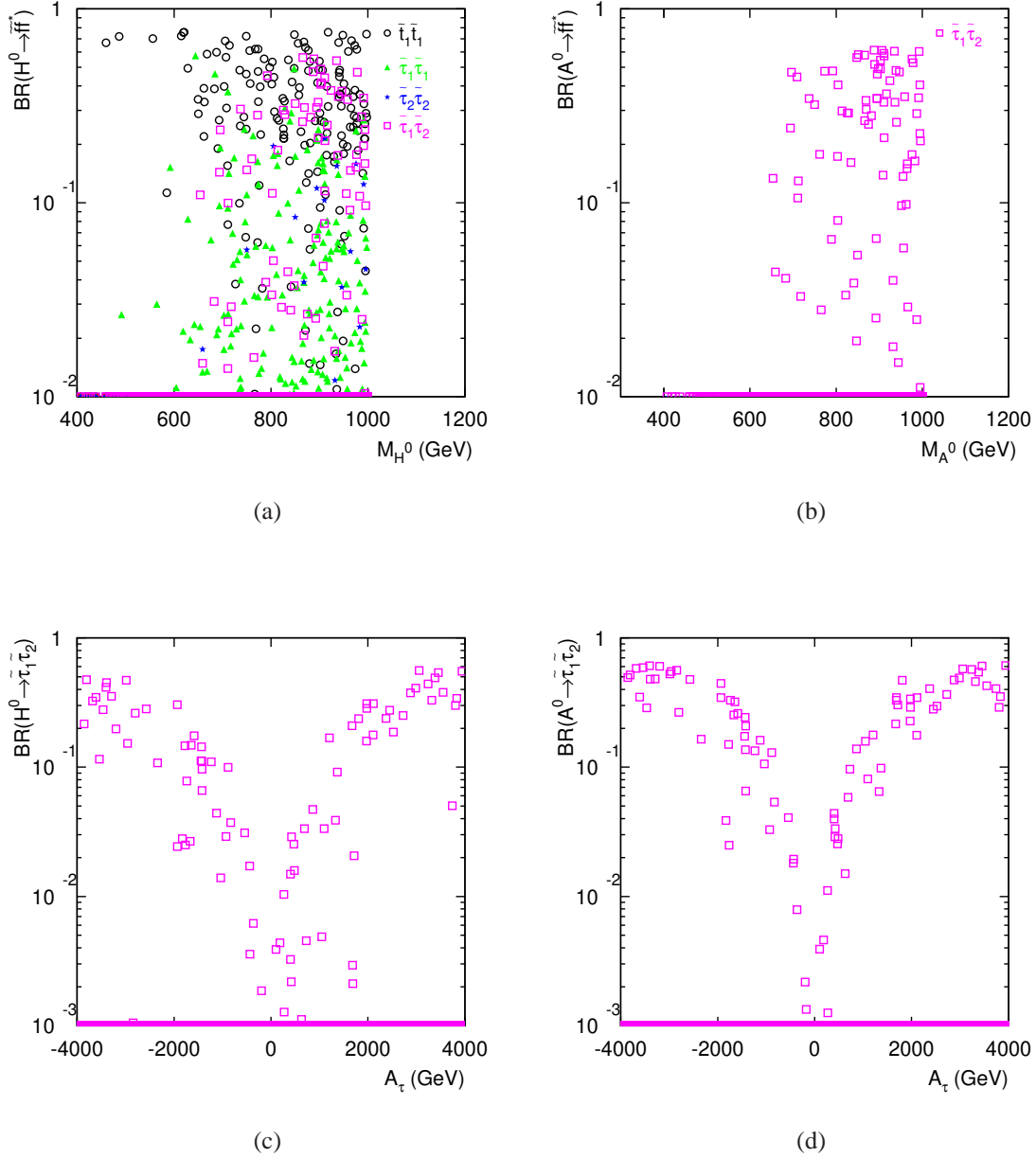


FIG. 10: (a) $BR(H^0 \rightarrow \tilde{f} \tilde{f}^*)$ vs. m_{H^0} , (b) $BR(A^0 \rightarrow \tilde{f} \tilde{f}^*)$ vs. m_{A^0} , (c) $BR(H^0 \rightarrow \tilde{\tau}_1 \tilde{\tau}_2^*)$ vs. A_τ and (d) $BR(A^0 \rightarrow \tilde{\tau}_1 \tilde{\tau}_2^*)$ vs. A_τ .

[hep-ph/0212020].

[15] S. Heinemeyer, W. Hollik and G. Weiglein, Eur. Phys. J. C **9**, 343 (1999) [hep-ph/9812472].

[16] M. Frank, T. Hahn, S. Heinemeyer, W. Hollik, H. Rzehak and G. Weiglein, JHEP **0702**, 047 (2007) [hep-ph/0611326], and references therein.

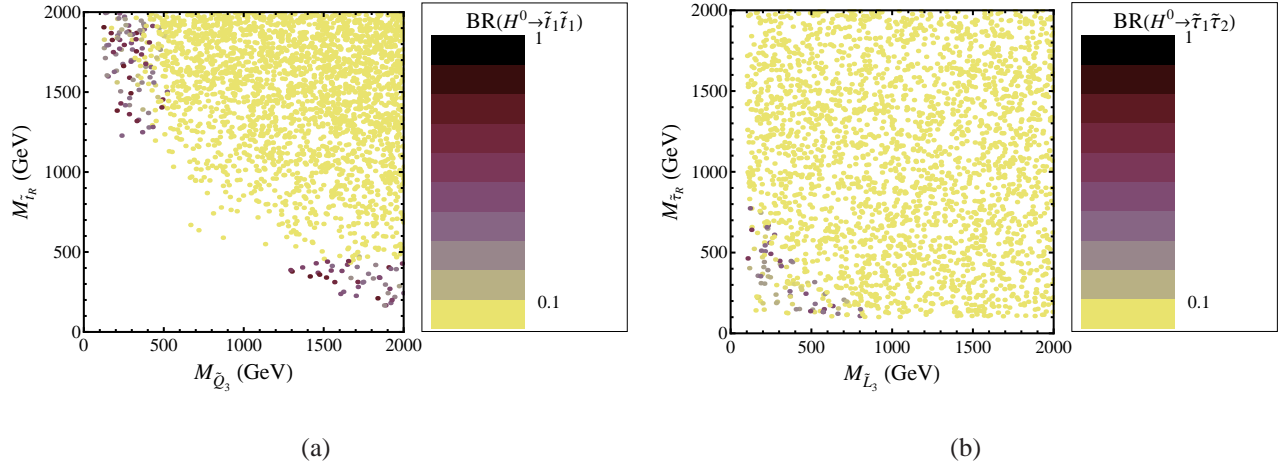


FIG. 11: (a) $BR(H^0 \rightarrow \tilde{t}_1 \tilde{t}_1^*)$ in the plane of $M_{\tilde{t}_R}$ vs. $M_{\tilde{Q}_3}$ and (b) $BR(H^0 \rightarrow \tilde{\tau}_1 \tilde{\tau}_2^* + \tilde{\tau}_2 \tilde{\tau}_1^*)$ in the plane of $M_{\tilde{\tau}_R}$ vs. $M_{\tilde{L}_3}$. The color scale gives the branching fraction of $H^0 \rightarrow \tilde{f} \tilde{f}^*$ decay.

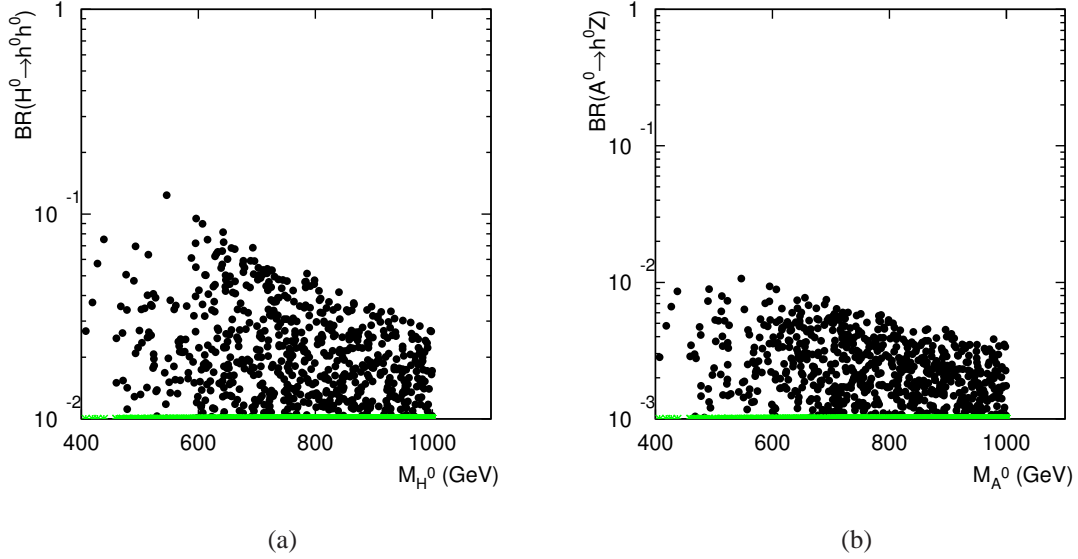


FIG. 12: (a) $BR(H^0 \rightarrow h^0 h^0)$ vs. m_{H^0} and (b) $BR(A^0 \rightarrow h^0 Z)$ vs. m_{A^0} .

[17] S. Heinemeyer, W. Hollik and G. Weiglein, Comput. Phys. Commun. **124**, 76 (2000) [hep-ph/9812320], and references therein.

[18] P. Bechtle, O. Brein, S. Heinemeyer, G. Weiglein and K. E. Williams, Comput. Phys. Commun. **181**,

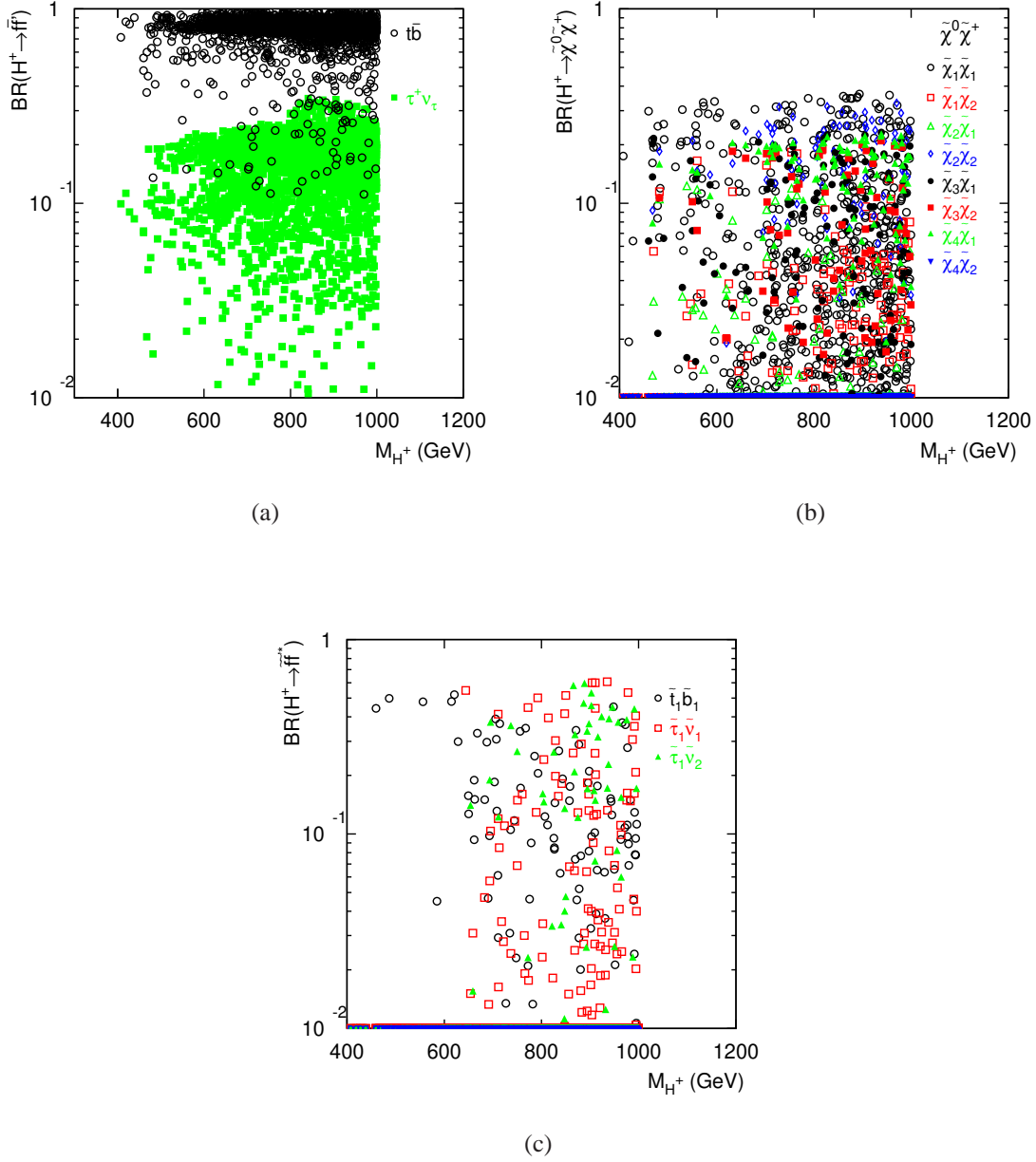


FIG. 13: (a) $BR(H^+ \rightarrow f \bar{f})$ vs. m_{H^+} , (b) $BR(H^+ \rightarrow \tilde{\chi}_i^0 \tilde{\chi}_j^+)$ vs. m_{H^+} and (c) $BR(H^+ \rightarrow f \tilde{f}'^*)$ vs. m_{H^+} .

138 (2010) [arXiv:0811.4169 [hep-ph]], and references therein; *ibid.*, Comput. Phys. Commun. **182**, 2605 (2011) [arXiv:1102.1898 [hep-ph]], and references therein.

[19] Combined results from the LEP2 experiments, Phys. Lett. B**565**, 61 (2003).

[20] T. Aaltonen *et al.* [CDF Collaboration], Phys. Rev. Lett. **103**, 101803 (2009) [arXiv:0907.1269 [hep-

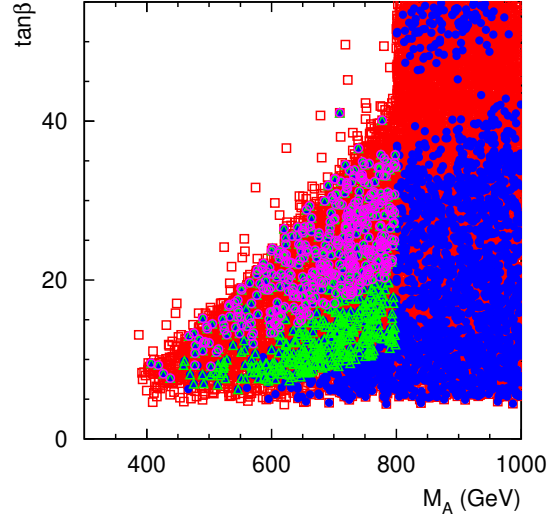


FIG. 14: Exclusion for $H^0/A^0 \rightarrow \tau\tau$ mode in the plane of $\tan\beta$ vs. m_A with $L = 300 \text{ fb}^{-1}$ (purple open circle) and 3000 fb^{-1} (green open triangle), based on surviving region in Fig. 1.

- ex]]; V. M. Abazov *et al.* [D0 Collaboration], Phys. Lett. B **682**, 278 (2009) [arXiv:0908.1811 [hep-ex]].
- [21] Y. Amhis *et al.* [Heavy Flavor Averaging Group Collaboration], arXiv:1207.1158 [hep-ex].
- [22] RAaij *et al.* [LHCb Collaboration], Phys. Rev. Lett. **110**, 021801 (2013) [arXiv:1211.2674 [Unknown]].
- [23] M. Misiak, H. M. Asatrian, K. Bieri, M. Czakon, A. Czarnecki, T. Ewerth, A. Ferroglia and P. Gambino *et al.*, Phys. Rev. Lett. **98**, 022002 (2007) [hep-ph/0609232]; T. Becher and M. Neubert, Phys. Rev. Lett. **98**, 022003 (2007) [hep-ph/0610067].
- [24] K. S. Babu and C. F. Kolda, Phys. Rev. Lett. **84**, 228 (2000) [hep-ph/9909476]; A. J. Buras, J. Girrbach, D. Guadagnoli and G. Isidori, Eur. Phys. J. C **72**, 2172 (2012) [arXiv:1208.0934 [hep-ph]].
- [25] M. Misiak and M. Steinhauser, Nucl. Phys. B **764**, 62 (2007) [hep-ph/0609241].
- [26] J. P. Lees *et al.* [BaBar Collaboration], Phys. Rev. Lett. **109**, 101802 (2012) [arXiv:1205.5442 [hep-ex]].
- [27] F. Mahmoudi, Comput. Phys. Commun. **178**, 745 (2008) [arXiv:0710.2067 [hep-ph]]; F. Mahmoudi, Comput. Phys. Commun. **180**, 1579 (2009) [arXiv:0808.3144 [hep-ph]]; F. Mahmoudi, Comput. Phys. Commun. **180**, 1718 (2009).

- [28] M. S. Carena, M. Quiros and C. E. M. Wagner, Nucl. Phys. B **461**, 407 (1996) [arXiv:hep-ph/9508343]; M. S. Carena, J. R. Espinosa, M. Quiros and C. E. M. Wagner, Phys. Lett. B **355**, 209 (1995) [arXiv:hep-ph/9504316].
- [29] M. Carena, S. Gori, N. R. Shah, C. E. M. Wagner and L. -T. Wang, JHEP **1308**, 087 (2013) [arXiv:1303.4414 [hep-ph]].
- [30] P. Bechtle, S. Heinemeyer, O. Stal, T. Stefaniak, G. Weiglein and L. Zeune, Eur. Phys. J. C **73:2354** (2013) [arXiv:1211.1955 [hep-ph]].
- [31] M. Carena, S. Gori, N. R. Shah and C. E. M. Wagner, JHEP **1203**, 014 (2012) [arXiv:1112.3336 [hep-ph]]. M. Carena, S. Gori, N. R. Shah, C. E. M. Wagner and L. -T. Wang, JHEP **1207**, 175 (2012) [arXiv:1205.5842 [hep-ph]].
- [32] K. Blum, R. T. D’Agnolo and J. Fan, JHEP **1301**, 057 (2013) [arXiv:1206.5303 [hep-ph]]; M. R. Buckley and D. Hooper, Phys. Rev. D **86**, 075008 (2012) [arXiv:1207.1445 [hep-ph]]; J. R. Espinosa, C. Grojean, V. Sanz and M. Trott, JHEP **1212**, 077 (2012) [arXiv:1207.7355 [hep-ph]].
- [33] G. Aad *et al.* [ATLAS Collaboration], ATLAS-CONF-2013-068.
- [34] G. Aad *et al.* [ATLAS Collaboration], arXiv:1308.2631 [hep-ex].
- [35] S. Chatrchyan *et al.* [CMS Collaboration], CMS PAS SUS-12-022.
- [36] C. Han, X. Ji, L. Wu, P. Wu and J. M. Yang, arXiv:1307.3790 [hep-ph]; Eric Brownson, Nathaniel Craig, Ulrich Heintz, Gena Kukartsev, Meenakshi Narain, and Neeti Parashar, presentation in Snowmass meeting, Minneapolis, 2013; B. Coleppa, F. Kling and S. Su, arXiv:1308.6201 [hep-ph].